Jetlike Component in Sputtering of LiF Induced by Swift Heavy Ions

M. Toulemonde,[1,2] W. Assmann,[2] C. Trautmann,[3] and F. Grüner[2]
[1]*CIRIL, CEA-CNRS-ISMRA, BP 5133, 14070 Caen cedex 5, France*
[2]*Sektion Physik, Ludwig-Maximilians-Universität München, 85748 Garching, Germany*
[3]*Gesellschaft für Schwerionenforschung, Planckstrasse 1, 64291 Darmstadt, Germany*
(Received 19 October 2001; published 22 January 2002)

Angular distributions of sputtered atoms from SiO_2 and LiF single crystals were measured under the irradiation of 1 MeV/u swift heavy ions. In contrast to the almost isotropic distribution of SiO_2, an additional jetlike component was observed for LiF. The total sputtering yield of SiO_2 ($\approx 10^2$ atoms/ion) can be reproduced by an extended inelastic thermal spike model, whereas the huge yield of LiF ($\approx 10^4$ atoms/ion) needs a substantial decrease of the sublimation energy to be described by the model.

DOI: 10.1103/PhysRevLett.88.057602 PACS numbers: 79.20.Rf, 61.80.Jh, 78.55.Fv, 82.80.Yc

When energetic heavy ions are slowing down in solids, they create along their trajectory a zone of intense electronic excitations confined to a cylindrical region of about 10 nm diameter. Projectiles in the MeV to GeV energy range typically deposit some 10 keV per nanometer path length inducing in many materials dramatic modifications at the surface and in the bulk. Examples are phase changes inside the tracks from the crystalline to the amorphous state [1] or from a superconductor to an insulator [2], the creation of a high temperature [3], high pressure [4], or high stress phase [5]. The characteristic track dimensions are well matched to the controlled production of structural modifications on a nm scale. This possibility has recently been used to create conducting tracks as field emitters in an insulating carbon matrix [6]. Although ion beams are already applied in many scientific and technological fields, there is still a lack of understanding concerning the complex processes involved in track formation.

The question of what mechanisms the energy deposited in electronic excitations is transferred into kinetic energy of the lattice atoms is still under discussion. Several track models based on different physical scenarios have been developed [1,4,7–9]. However, since track formation occurs within a time of 10^{-12} s and within a confined volume of some nm^3, the dynamic process of atomic motion cannot be observed directly in the bulk of the target material. Whatever mechanism dominates the track formation, it should also govern the sputtering at the sample surface [10]. Sputtering data in the electronic energy loss regime are available for different materials [10–16] but total sputtering yields have not been linked to related bulk observations so far. For this purpose, a series of new sputtering experiments have been performed on two different types of insulators, single crystalline LiF and SiO_2 (α quartz). In both cases, track formation in the bulk has been studied in great detail [1,17–20] and described in the framework of an inelastic two-temperatures thermal spike model [7]. A suitable model should allow a consistent description of surface and bulk observations with the same set of parameters.

In this Letter, we report new and unexpected sputtering of LiF seen both in the total yield and in the angular distribution. While sputtering of Si particles from quartz is nearly isotropic, typical for a thermal process [13,15], Li and F exhibit an additional sharp jetlike component symmetric around the surface normal. Such a peak has till now never been seen for bulk crystals, only for nanocrystalline Au targets [21]. Moreover, the total yield of LiF reaches values around 10^4 sputtered particles per incident ion, almost 2 orders of magnitude larger than for SiO_2. This huge yield is well beyond collisional cascade sputtering expectations and rules out any crystalline orientation effect (Wehner spots). It is shown that the total yield of SiO_2 can be reproduced by the inelastic thermal spike model with parameters as deduced for tracks in bulk material [7]. In LiF, the binding energy has been lowered to describe the huge sputtering yield [9,22–24].

The sputtering experiments were performed at the Munich accelerator laboratory using S, Ni, I, and Au ions with different electronic stopping powers (see Table I) but roughly the same specific energy (≈ 1 MeV/u) in order to avoid the velocity effect [25]. To reach equilibrium charge states, all projectiles passed through a thin carbon foil in front of the sputter samples. The beam incidence angle α was either rather flat ($\alpha = 19°$) or more normal ($60° < \alpha < 75°$) with respect to the sample surface (see Fig. 1). The typical spot size was 10 mm^2 ($\alpha = 19°$) or 3 mm^2 ($60° < \alpha < 75°$). The ion fluence was controlled via current measurements on the carbon foil, calibrated by a Faraday cup. Radiation damage of the sample surface was minimized by moving the samples and collecting sputtered particles from several irradiation spots, each of them limited to a maximum fluence of 2×10^{12} ions/cm^2 for LiF and 1×10^{13} ions/cm^2 for SiO_2. Sputtered atoms emitted from the target surface were collected on arc-shaped catcher foils of high purity Al or Cu, mounted perpendicular to the incident beam. In some cases, a second arc was added parallel to the beam to check the azimuthal symmetry of the angular distribution. After irradiation, the area density of the particles sputtered onto each catcher foil was

TABLE I. Parameters of sputtering experiments and results. E_i is the incident energy, dE/dx the initial energy loss, and α the incidence angle of the beam with respect to the sample surface. Y_{tot} is the total yield of the specified atom per incoming ion; the experimental errors are less than 20% (in some cases F detection was inhibited due to catcher oxidation). σ and Y_a denote the width and partial yield of the anisotropic component, respectively.

Target	Ion	E_i (MeV)	dE/dx (keV/nm)	α (deg)	Sputter species	Y_{tot} (at/ion)	σ (rad)	Y_a
SiO_2	Au	210	21.9	19	Si	1000		
	I	150	16.4	19	Si	530		
LiF	Au	210	21.5	19	F	45 590	0.35	20 130
					Li	41 220	0.37	20 300
	I	150	16.2	19	F	15 790	0.51	12 010
					Li	17 530	0.47	11 380
	Ni	70	10.4	19	F	2210	0.17	210
					Li	1990	0.21	320
	S	50	5.0	19	Li	120	0.19	15
LiF	Au	210	21.5	70	F	10 260	0.14	1280
					Li	9630	0.13	850
				60	Li	5060	0.16	660
	I	150	16.2	75	F	1940	0.22	350
					Li	1890	0.30	470
	Ni	70	10.4	70	Li	270	0.26	60

analyzed by means of elastic recoil detection analysis available in the same irradiation chamber [26]. To protect the collected atoms from being sputtered off by the analyzing 150 MeV Au ion beam, the catcher foils were covered by a thin Cu layer. From a step by step analysis along the full length of the catcher, the differential sputter yields $dY(\theta)/d\Omega$ of F, Li, and Si were determined as a function of the sputtering angle θ. In a separate experiment, measuring the total sputtering yield by the thickness decrease of a thin LiF layer, the sticking coefficient on the catcher was found to be close to one.

For all ion beams, LiF exhibits stoichiometric sputtering within the experimental errors of 20% (Y_{tot} in Table I). The corresponding behavior of SiO_2 could not be determined due to unavoidable surface oxidation of the catcher material. The angular distribution of Si follows a slightly over-cosine function $\cos^n\theta$ with $n \approx 1.3$. This is in remarkable contrast to LiF where both atom species are strongly peaked around the surface normal with azimuthal symmetry superimposed on a cosine background (Figs. 1 and 2). This jetlike anisotropy occurs more or less pronounced for all beam incidence angles and for perpendicular as well as parallel beam-catcher orientation. A good fit for this angular distribution is given by a two-component function $dY(\theta)/d\Omega = A\cos\theta + Be^{-\theta^2/\sigma^2}$. Using this fit function, the total sputtering yield Y_{tot}, the contribution of

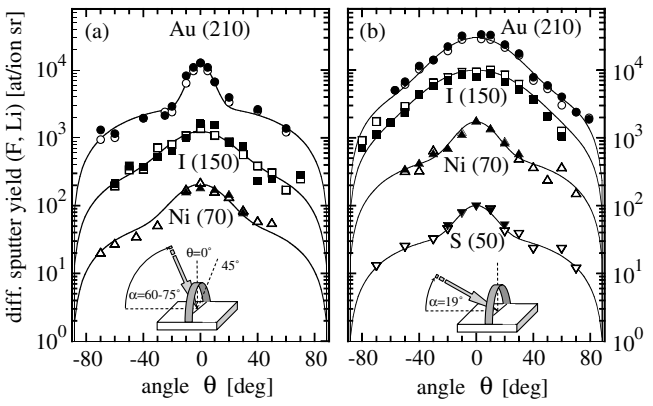

FIG. 1. Angular distribution of sputtered Li (open symbols) and F (filled symbols) atoms for irradiation with various ions (energy given in MeV) at beam incidence (a) close to normal ($60° < \alpha < 75°$) and (b) flat incidence ($\alpha = 19°$). In some cases, F data are missing at large angles due to surface oxidation of the catcher.

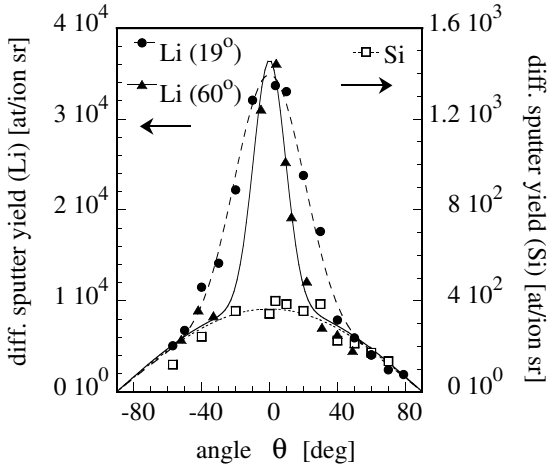

FIG. 2. Angular distribution from SiO_2 and LiF irradiated with 210 MeV Au ions: Si yield at $\alpha = 19°$ (squares), Li yield at $\alpha = 19°$ (circles), and at $\alpha = 60°$ (triangles), the latter multiplied by 6.8 for better comparison.

the jet, and the angular halfwidth were calculated (Table I). Note that the angular halfwidth of the anisotropic component as a function of the energy loss decreases for flat incidence and increases for normal incidence. The total yield of LiF is huge, 2 orders of magnitude larger than for SiO_2. For flat incidence of the beam ($\alpha = 19°$), Y_{tot} is on the average 8 times larger than for normal incidence ($60° < \alpha < 75°$) which is more than expected from a $\sin\alpha^{-1}$ law. We find a $\sin\alpha^{-1.85}$ which is quite in agreement with the observations made for sputtering of frozen O_2 [27]. For LiF, the Y_{tot} follows a dE/dx power law with an exponent between 4 and 5 (Fig. 3) for all incident angles α. Extrapolation of the data for both incidence angles to low dE/dx values gives a sputter threshold around 5(2) keV/nm for LiF and 9(2) keV/nm for SiO_2.

Large non-nuclear sputtering yields are well known from insulators in the electronic stopping power regime and several qualitative models have been proposed [12]. None of them, however, neither analytical macroscopic [13–15,28–30] nor defect-mediated sputtering models [31], can explain the present behavior of LiF. Only molecular dynamics calculations can reproduce peaked angular distributions [32–34], a dE/dx evolution of the sputtering yield with a power law, larger than 3, and the evolution of the sputtering yield versus the irradiation angle [32–34]. But at present this microscopic description is not developed for ionic crystals.

Coming back to our results, the isotropic emission of particles suggests a thermal process [13–15]. We therefore applied the existing inelastic thermal spike model [7], in which we have included the surface evaporation for a quantitative description of our data. The numerical solution of the two coupled differential equations governing the heat diffusion in the electron and lattice subsystems allows us to calculate the evolution of the temperature T_a of the bulk lattice versus time (t) and space (r). The total yield Y_{tot} of particles evaporated from the surface is then determined by integrating the evaporation rate Φ [15,35] as a function of $T_a(t, r)$:

$$Y_{tot} = \int dt \int dr\, \Phi(T_a(t, r)) \tag{1}$$

and

$$\Phi(T_a(t, r)) = N\sqrt{\frac{kT_a(t, r)}{2\pi M}}\exp\left(\frac{-U}{kT_a(t, r)}\right), \tag{2}$$

where N is the atomic density, k is the Boltzmann constant, and M is the molecular mass of the target. The surface binding energy U is assumed to be equal to the sublimation energy per evaporated molecule. For temperatures above vaporization, the temperature dependence of the thermal diffusivity [35] was used. The model calculations also included the possible scenario of superheating. In such a situation, the latent heat during the liquid-vapor phase transition was ignored leading to higher temperatures but also to faster cooling rates. All calculations were performed for tracks oriented perpendicular to the target surface. For the electron-phonon coupling constant λ of quartz we used a value of 3.6 deduced earlier from thermal spike calculations of a large set of track radii in bulk material [1,20], assuming that amorphization occurs by quenching of a melt phase. Figure 3a shows the experimental sputtering data, normalized to normal incidence by $\sin\alpha^{-1.85}$, together with the calculated results using the known sublimation energy of $U = 5.4$ eV per molecule. Assuming superheating, the thermal spike model can obviously predict the total yield in quartz within the correct order of magnitude. Moreover, independent of the parameters of the vapor phase, the calculated sputtering threshold is around $dE/dx \approx 10$ keV/nm, in good agreement with the experimental data.

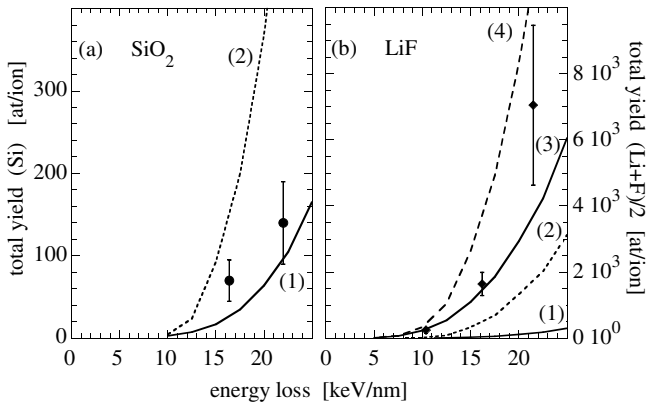

FIG. 3. Total sputtering yield per incoming ion as a function of energy loss for (a) SiO_2 irradiated at $\alpha = 19°$ and (b) LiF irradiated at $60° < \alpha < 70°$. All Y_{tot} values were divided by $\sin\alpha^{-1.85}$. Curves (1) and (3) assume superheating. For LiF, the binding energy for curves (1) and (2) is 2.8 eV, and that for curves (3) and (4) is 1.3 eV.

In the case of LiF, the sputtering process, measured under normal beam incidence, is obviously dominated by the isotropic cosine component supporting also a thermal process. In a first approach, Y_{tot} was estimated within the inelastic thermal spike model using $\lambda = 3.8$ nm. With this value bulk tracks can be described [7,17] assuming formation by quenching of a "vapor phase," i.e., by rapid cooling of atoms which have surpassed the known sublimation energy of $U = 2.8$ eV per molecule. Figure 3b presents the calculated sputter yields with (curve 1) and without (curve 2) superheating. Neither the total yield nor the experimental sputtering threshold (5 keV/nm) can be reproduced by this parameter set. It has been suggested that the high density of excitation and ionization along the ion path leads to a pronounced instability of the interatomic bonds [9,22–24] and thereby to a decrease of the surface binding energy. As a first approach, we performed additional thermal spike calculations with a lower sublimation energy. A value $U = 1.3$ eV per molecule (Fig. 3b) gives

the best agreement at normal incidence for both Y_{tot} and its dE/dx dependence. However, it is clear that such an approach cannot describe any anisotropic angular distribution. At this stage, we can speculate on a hydrodynamic process driven by the pressure induced by the vapor phase [7]. At first, the appearance of a gas phase would induce radial pressure in the track core released by a jet of atoms from the impact area. In a later stage, evaporation from a larger heated track zone leads to an isotropic distribution. The beam incidence strongly influences the geometry of the impact zone and track formation at the surface. Under flat incidence, the radial pressure can easier relax towards the surface, leading to an increase of the anisotropic component Y_a (see Table I), whereas under normal incidence the heated atoms are more confined by the surrounding lattice. Groves, seen in LiF surfaces after irradiation at grazing incidence [36], and hillocks at normal incidence [17] support such a scenario.

In conclusion, for the first time a comprehensive data set is presented for sputter processes induced by heavy ions in the electronic stopping regime for two different insulators. From a SiO_2 quartz surface, Si atoms are emitted almost isotropically, and the total yield can be described by the inelastic thermal spike model using the same parameters as for track formation in the bulk. Crystalline LiF shows rather different behavior, exhibiting an additional jetlike anisotropic component possibly linked to a hydrodynamic process due to a vapor phase in the bulk. This may be a more general behavior as we have indications also for other ionic crystals such as CaF_2 and NaCl. The inelastic thermal spike model can describe the total sputtering yield, its evolution as a function of dE/dx, and the sputtering threshold assuming a largely reduced surface potential. This strong decrease of the molecule binding energy is possibly linked to the ionic character of LiF or the emission of clusters.

[1] A. Meftah *et al.,* Phys. Rev. B **49**, 12 457 (1994).
[2] H. Walter *et al.,* Phys. Rev. Lett. **80**, 3598 (1998).
[3] W. Assmann *et al.,* Nucl. Instrum. Methods Phys. Res., Sect. B **146**, 271 (1998).
[4] H. Dammak, A. Barbu, A. Dunlop, D. Leseur, and N. Lorenzelli, Philos. Mag. Lett. **67**, 253 (1993).
[5] C. Trautmann, S. Klaumünzer, and H. Trinkaus, Phys. Rev. Lett. **85**, 3648 (2000).
[6] M. Waiblinger *et al.,* Appl. Phys. A **69**, 239 (1999).
[7] M. Toulemonde, Ch. Dufour, A. Meftah, and E. Paumier, Nucl. Instrum. Methods Phys. Res., Sect. B **166/167**, 903 (2000).
[8] R. L. Fleischer, P. B. Price, and R. M. Walker, *Nuclear Tracks in Solids* (University of California Press, Berkeley, 1975).
[9] C. C. Watson and T. A. Tombrello, Radiat. Eff. **89**, 263 (1985).
[10] T. A. Tombrello, Nucl. Instrum. Methods Phys. Res., Sect. B **2**, 555 (1984).
[11] W. L. Brown, L. J. Lanzerotti, J. M. Poate, and W. M. Augustyniak, Phys. Rev. Lett. **40**, 1027 (1978).
[12] Special issue on *Fundamental Processes in Sputtering of Atoms and Molecules (SPUT92),* edited by P. Sigmund [Mat. Fys. Medd. **43** (1993)].
[13] J. E. Griffith, R. A. Weller, L. E. Seiberling, and T. A. Tombrello, Radiat. Eff. **51**, 223 (1980).
[14] C. K. Meins *et al.,* Radiat. Eff. **71**, 13 (1983).
[15] L. E. Seiberling, J. E. Griffith, and T. A. Tombrello, Radiat. Eff. **52**, 201 (1980).
[16] A. Meftah, M. Djebara, J. P. Stoquert, F. Studer, and M. Toulemonde, Nucl. Instrum. Methods Phys. Res., Sect. B **107**, 242 (1996).
[17] C. Trautmann, M. Toulemonde, K. Schwartz, J. M. Costantini, and A. Müller, Nucl. Instrum. Methods Phys. Res., Sect. B **164/165**, 365 (2000).
[18] K. Schwartz, C. Trautmann, T. Steckenreiter, O. Geiss, and M. Krämer, Phys. Rev. B **58**, 11 232 (1998).
[19] C. Trautmann, M. Toulemonde, J. M. Costantini, J. J. Grob, and K. Schwartz, Phys. Rev. B **62**, 13 (2000).
[20] M. Toulemonde *et al.,* Nucl. Instrum. Methods Phys. Res., Sect. B **178**, 331 (2001).
[21] I. A. Baranov, Yu. V. Martynenko, S. O. Tsepelevich, and Yu. N. Yavlinskii, Sov. Phys. Usp. **31**, 1015 (1988).
[22] P. Stampfli and K. H. Bennemann, Appl. Phys. A **60**, 191 (1995).
[23] J. Bok, J. Phys. C **5**, 3 (1983).
[24] G. S. Khoo, C. K. Ong, and N. Itoh, J. Phys. **5**, 1187 (1993).
[25] J. A. M. Pereira and E. F. da Silveira, Phys. Rev. Lett. **84**, 5904 (2000).
[26] W. Assmann *et al.,* Nucl. Instrum. Methods Phys. Res., Sect. B **89**, 131 (1994).
[27] K. M. Gibbs, W. L. Brown, and R. E. Johnson, Phys. Rev. B **38**, 11 001 (1988).
[28] R. E. Johnson and R. Evatt, Radiat. Eff. **52**, 187 (1980).
[29] H. M. Urbassek and J. Michl, Nucl. Instrum. Methods Phys. Res., Sect. B **122**, 427 (1997).
[30] R. E. Johnson, B. U. R. Sundqvist, A. Hedin, and D. Fenyo, Phys. Rev. B **40**, 49 (1989).
[31] J. A. M. Pereira and E. F. Da Silveira, Nucl. Instrum. Methods Phys. Res., Sect. B **127/128**, 157 (1997).
[32] H. M. Urbassek, H. Kafemann, and R. E. Johnson, Phys. Rev. B **49**, 786 (1994).
[33] E. M. Bringa, R. E. Johnson, and L. Dutkiewicz, Nucl. Instrum. Methods Phys. Res., Sect. B **152**, 267 (1999).
[34] E. M. Bringa and R. E. Johnson, Nucl. Instrum. Methods Phys. Res., Sect. B **180**, 99 (2001).
[35] P. Sigmund and C. Claussen, J. Appl. Phys. **52**, 2 (1981).
[36] I. V. Vorobyova, Nucl. Instrum. Methods Phys. Res., Sect. B **146**, 379 (1998).